

## Research Article

# Platelet Ultrastructural Morphology and Morphometry in 10 Patients with MYH9-Related Disease

Núria Pujol-Moix<sup>1-3\*</sup>, Ignacio Español<sup>4</sup>, Angel Hernández<sup>1</sup>, Miquel Vázquez-Santiago<sup>2,5</sup>, Joan-Carles Souto<sup>2,5</sup>, and Eduardo Muñoz-Díaz Eduardo<sup>6</sup>

<sup>1</sup>Platelet Pathology Unit, Hospital de la Santa Creu i Sant Pau, Spain

<sup>2</sup>Sant Pau Biomedical Research Institute (IIB Sant Pau), Spain

<sup>3</sup>Department of Medicine, University of Barcelona, Spain

<sup>4</sup>Hematology Department, Hospital Universitario Santa Lucía, Spain

<sup>5</sup>Unit of Hemostasis Thrombosis, Hospital of the Holy Cross and St. Paul, Spain

<sup>6</sup>Blood and Tissue Bank, Barcelona, Spain

**\*Corresponding author**

Núria Pujol-Moix, Institut d'Investigació Biomèdica Sant Pau (IIB Sant Pau), Hospital de la Santa Creu i Sant Pau, Av. Sant Antoni M. Claret, 16708025-Barcelona, Spain, Tel: 34-935-537-151; Fax: 34-93-5537-153; Email: npujolmoix@gmail.com

Submitted: 29 June 2017

Accepted: 22 August 2017

Published: 25 August 2017

ISSN: 2333-6684

Copyright

© 2017 Pujol-Moix et al.

**OPEN ACCESS****Keywords**

- MYH9-related disease
- Giant platelets
- Platelet ultrastructure
- Morphometry
- Membrane complexes

**Abstract**

MYH9-related disease is an autosomal dominant hereditary macro thrombocytopenia caused by mutations in the *MYH9* gene which encodes the non-muscular myosin heavy chain type IIA. The patients have mild clinical bleeding, grayish-blue inclusions in granulocytes and, in some cases, nephropathy, neurosensory deafness, and cataracts. The aim of our study was to assess the platelet ultra structure in MYH9-related disease with the help of morphometry.

Ten patients with genetically confirmed MYH9-related disease were studied together with a group of 15 healthy individuals. The ultra structure of a minimum of 150 platelet sections for each patient was examined, and the morphometry of the main platelet traits was performed. We measured the size and shape of resting platelets, the diameter, number per platelet and number per unit of platelet area of the granules, dense bodies, mitochondria and lipid droplets. Moreover, we measured the percentage of platelet area occupied by open canalicular system and by glycogen masses. We compare the results between patients and controls using the one-way analysis of variance.

We confirmed that MYH9-RD platelets are larger and rounder than normal platelets and they show expanded open canalicular system and increased membrane complexes. Moreover, we found that the size of  $\alpha$ -granules and dense bodies was enlarged, and the amounts of mitochondria and glycogen, both related to cell energy metabolism, were significantly increased.

**ABBREVIATIONS**

MYH9-RD: MYH9-related disease; NMMHC-IIA: Non-Muscular Myosin Heavy Chain Iia; CDI: Circular Deviation Index; OCS: Open Canalicular System; DTS: Dense Tubular System

**INTRODUCTION**

MYH9-related disease (MYH9-RD) is an autosomal dominant genetic platelet disorder characterized by mild clinical bleeding, thrombocytopenia with giant platelets and grayish-blue cytoplasmic inclusions in granulocytes. Extra-hematological pathologies are also present in some cases including neurosensory deafness, nephropathy and/or cataracts. The disease is caused by mutations in the *MYH9* gene which encodes the non-muscle myosin heavy chain IIA (NMMHC-IIA) [1,2]. The presence of the abnormal protein in platelet cytoskeleton disturbs the composition and contractile functions of this structure [3,4]. In megakaryocytes, the abnormal protein causes changes in cytoskeletal mechanics and in demarcation membranes that leads to defective proplatelet formation [5-7].

Thus, megakaryocytes produce decreased number of platelets of increased volume but it has been suggested that the total platelet mass is preserved [8,9].

The platelets of the MYH9-RD patients observed by transmission electron microscopy have generally been described as normal except for their large size. The presence of a special type of membrane complexes and disorganization of the microtubules have also been reported [10,11]. The aim of the present study was to analyze the platelet ultra structure of 10 patients with MYH9-RD and to compare the results with those of a group of healthy individuals. In normal individuals, there is strong variability in the intraplatelet structure, which is even greater when observe in ultrathin sections because of random sectioning. Therefore, we studied a big number of platelet sections and applied morphometric methods to obtain quantitative results suitable for statistical analysis.

**MATERIALS AND METHODS**

Ten patients with genetically confirmed MYH9-RD, from

5 unrelated families, were enrolled in the study (Table 1). The ultra structure of the granulocyte inclusions as well as the *MYH9* gene mutations of these patients were previously published [12]; here we have used the same individual and family identifications that in the previous article. Fifteen healthy individuals were included in the study as controls. In all patients, a careful clinical evaluation and a complete family history was undertaken. This included a detailed estimation of bleeding and the investigation of extra-hematological manifestations such as nephropathy, neurosensory deafness and cataracts. Standard hematological and biochemical tests were performed, together with evaluation of kidney function, hearing and sight.

Blood platelet counts were determined by standard electronic cell counters and by phase contrast microscopy; a number  $\geq 150 \times 10^9/L$  was considered normal. Air-dried blood films, directly taken without anticoagulant and stained with May-Grünwald-Giemsa, were observed by light microscopy to assess the size and morphology of the platelets and the granulocyte cytoplasmic inclusions. Platelets with a diameter equal or greater than half a red blood cell (approximately  $\geq 4 \mu m$ ) were considered giant.

The platelet processing for transmission electron microscopy was carried out as previously described [13]. Briefly: to obtain resting platelets, fresh venous blood without anticoagulant was immediately fixed in 1.25 % glutaraldehyde in White's saline previously heated to 37°C. The platelet pellets were recovered and post-fixed in 1 % osmium tetroxide in White's saline. Then, they were dehydrated in alcohol and embedded in Epon 812 following standard methods. The ultrathin sections were stained with uranyl acetate and lead citrate before being examined in a transmission electron microscope at 80 Kv accelerating voltage. The observation at 12,000 magnification of one high quality ultrathin cut was generally sufficient to obtain 6 to 8 digital photos with a total of 150 different platelet sections or more. A cross-grating replica was photographed before and after the takes to perfect the exact magnification of the images.

Two-dimensional morphometry was performed on the platelet images using the computer- assisted image analysis software Nis-Elements BR 3.10 (Nikon, Tokyo, Japan). Based on the identification of platelets and their organelles, according with previous morphological descriptions, the following parameters were measured:

- Platelets: area, maximum diameter and circular deviation index ( $CDI = 4\pi \times \text{area} / \text{perimeter}^2$ ); this index indicates the discoid shape of platelet sections: the more rounded the shape the higher the CDI

- Platelet  $\alpha$ -granules, dense-bodies, mitochondria and lipid droplets: diameter, number per platelet and number per  $\mu m^2$  of platelet area

- Open canalicular system (OCS): area of individual channels and total area with respect to the platelet area %

- Clusters of OCS and DTS channels, and membrane complexes (formed by OCS and DTS channels): number per platelet and number per  $\mu m^2$  of platelet area

- Glycogen masses: total area with respect to the platelet area %

The results were expressed as mean  $\pm$  standard deviation. The one-way analysis of variance was used to compare means between measures of patients and controls; p-values of  $\leq 0.05$  were considered to indicate statistical significance.

The morphology of the measured structures was also assessed as well as the morphology of other platelet structures not suitable for morphometry such as DTS or microtubules.

## RESULTS AND DISCUSSION

The mean age of the patients at diagnosis was 47 years with a range between 12 and 78, and there were 6 women and 4 men (Table 1). An autosomal dominant hereditary pattern was observed in all families, which showed the same *MYH9* gene mutation in all the affected members. Four individuals from 2 families had progressive neurosensory deafness but none had nephropathy or pre-senile cataracts. The mutations found in these families were R1165 and D1424 in the coiled coil, a region associated with intermediate frequency of extra-hematological phenotypes [2,14]. The mutations found in the other 3 families were E1841K and R1933X in the C-terminal nonhelical tail which usually gives blood cell abnormalities only [14]. The bleeding symptoms were irregular, even in the same family as reported previously [1,11], and the most frequently observed were easy bruising and menstrual bleeding. Four women had excessive bleeding in some, but not all, their deliveries. On the other hand, in 5 patients (A2, B4, C6, D8, D9) the thrombocytopenia was an incidental finding as in other cases reported [1,11,15].

Using standard electronic cell counters, all patients presented different degrees of thrombocytopenia (Table 1). However, the microscopic counts always gave a much higher number of platelets, almost normal or even normal in some cases. This is because, in electronic counters, giant platelets exceed the upper threshold of platelet volumes and, therefore, they are not included in the platelet count or in the mean platelet volume [15,16]. For this reason, we provide here the microscopic counts in addition to the electronic counts. In contrast, we do not provide the mean platelet volumes because either the electronic counter did not give them or it gave values that clearly did not reflect the large platelet sizes. By light microscopy, all our patients showed platelets enlarged in size and a variable proportion of granulocytes with grayish-blue cytoplasmic inclusions (Figure 1) which we described in detail in a previous article [12]. Platelet macrocytosis was generalized with a few proportions of small platelets. There was a variable proportion of giant platelets reaching some of them the size of red blood cells or even more, similarly to other reported cases [8,11,17-23]. The patient's platelets were generally round or oval and occasionally elongated, and the platelet color was generally normal with the presence of occasional vacuoles as it has been described in other published cases [11].

The platelets observed by transmission electron microscopy exhibited characteristic ultrastructural traits (Figure 2) which were confirmed by morphometry (Table 2). The patients' mean platelet area and maximum diameter were significantly enlarged compared to the controls, and the circular deviation index (CDI) was increased, indicating that the platelets tended to be rounder rather than discoid. The previous reports on platelet ultra structure of *MYH9*-RD generally described it as normal, apart

**Table 1:** Patients with MYH9-related disease: clinical and laboratory data and MYH9 gene mutations.

Family Case	Familial relationship	Age Sex	MYH9 gene mutation	Deafness	Bleeding					Platelet counts (x10 <sup>9</sup> /L)		Giant platelets (%)	Granulocytes With inclusions (%)
					EB	Ep	Me	Su	Ob	elec-tronic	micro-scopic		
A1	proband	53 F	E1841K, exon 39	-	+	+	++	++	2/3	35	80	62	92
A2	mother	78 F	nd	-	-	-	-	na	0/2	75	130	25	98
B3	proband	30 F	R1933X, exon 40	-	+	-	+	-	0/1	13	90	21	69
B4	mother	55 F	R1933X, exon 40	-	+	-	+	-	0/2	40	94	7	61
C5	proband	38 F	R1933X, exon 40	-	±	-	-	-	1/4	35	87	12	74
C6	son	12 M	R1933X, exon 40	-	-	-	na	na	na	24	93	31	69
D7	proband	70 F	R1165C, exon 26	++	+	-	-	-	1/3	75	154	15	46
D8	daughter	33 F	R1165C, exon 26	±	+	-	-	na	1/1	68	85	15	47
D9	daughter	44 F	R1165C, exon 26	+	+	-	±	-	0/2	81	153	13	67
E10	proband	58 M	D1424Y, exon 31	++	-	±	na	-	na	16	60	53	95

**Table 2:** Platelet ultra structural morphometry: comparative results between patients with MYH9-related disease and healthy controls.

	Controls (n= 15) mean (SD)	Patients (n = 12) mean (SD)	P value
<b>Platelets</b>			
area (µm <sup>2</sup> )	1.64 (0.29)	3.92 (0.72)	<0.0001
maximum diameter (µm)	2.25 (0.20)	2.97 (0.31)	<0.0001
circular deviation index	0.62 (0.03)	0.66 (0.05)	0.0152
<b>Platelet specific granules</b>			
α-granules, diameter	181 (27)	210 (33)	0.0284
α-granules, number per platelet	5.02 (0.56)	8.95 (3.84)	0.0002
α-granules, number per µm <sup>2</sup> of platelet area	3.15 (0.72)	2.25 (0.46)	0.6574
dense bodies, diameter	222 (29)	243 (40)	0.0052
dense-bodies, number per platelet	0.42 (0.13)	1.08 (0.31)	0.0001
dense-bodies, number per µm <sup>2</sup> of platelet area	0.24 (0.05)	0.262 (0.097)	0.1520
<b>Platelet membrane structures</b>			
OCS, area of individual channels	0.014 (0.002)	0.017 (0.426)	0.0470
OCS, total area % of platelet area	5.31 (0.95)	8.10 (1.94)	0.0049
OCS-clusters, number per platelet	0.028 (0.032)	0.027 (0.036)	0.9440
OCS-clusters, number per µm <sup>2</sup> of platelet area	0.017 (0.019)	0.010 (0.019)	0.8792
DTS-clusters, number per platelet	0.023 (0.028)	0.034 (0.040)	0.0984
DTS-clusters, number per µm <sup>2</sup> of platelet area	0.014 (0.017)	0.085 (0.093)	0.0794
MC, number per platelet	0.016 (0.014)	0.171 (0.063)	<0.0001
MC, number per µm <sup>2</sup> of platelet area	0.010 (0.008)	0.043 (0.018)	0.0049
<b>Other intraplatelet structures</b>			
mitochondria, diameter	215 (35)	258 (47)	0.0023
Mitochondria, number per platelet	0.41 (0.21)	1.17 (0.51)	0.0001
Mitochondria, number per µm <sup>2</sup> of platelet area	0.265 (0.080)	0.314 (0.221)	0.0280
lipid droplets, diameter	315 (76)	342 (92)	0.4306
lipid droplets, number per platelet	0.023 (0.028)	0.0160 (0.095)	0.0420
lipid droplets, number per µm <sup>2</sup> of platelet area	0.036 (0.044)	0.0390 (0.032)	0.1060
glycogen, total area % of platelet area	1.82 (0.35)	2.84 (0.96)	0.0176

**Abbreviations:** SD: Standard Deviation; OCS: Open Canalicular System; DTS: Dense Tubular System; MC: Membrane Complexes

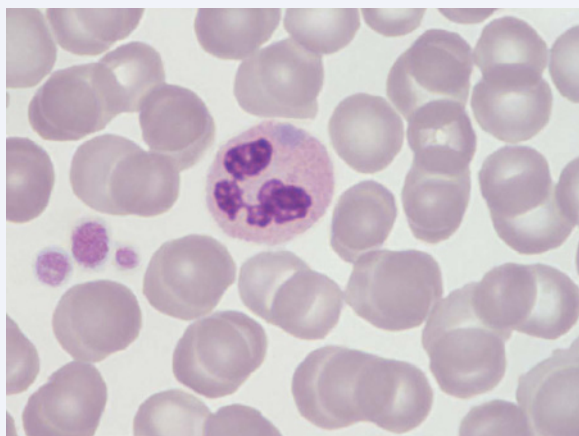


**Figure 1** Air-dried blood film showing one neutrophil granulocyte with a graysh-blue cytoplasmic inclusion and three macrocytic platelets. May-Grünwald-Giemsa, x 1000.

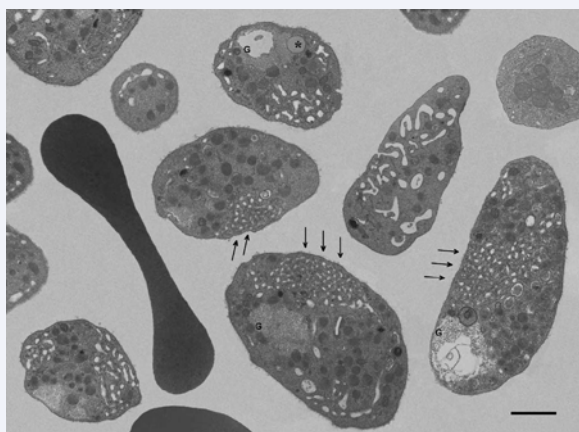


**Figure 2** Several platelet sections, which are larger and rounder than normal, and one red blood cell section. Platelets show expanded open canalicular system, abundant membrane complexes, which are typical of MYH9-disease (arrows), and normal appearing  $\alpha$ -granules, dense bodies and mitochondria. Platelets also show several masses of glycogen (G) and a lipid droplet (asterisk). Transmission electron microscopy; bar = 2.5  $\mu$ m.

from the enlarged platelet size [8,11,18,19,24,25]. Other authors observed that the microtubules were dispersed in the platelet cytoplasm instead of to be organized in an equatorial marginal band [10,15,21,22]. As this marginal band is the major support system for maintaining the platelet resting discoid shape, it has been suggested that the more spherical shape of giant platelets may be due to the dispersion of the microtubules outside the band [26].

The diameters of  $\alpha$ -granules and dense-bodies were significantly larger in our patients (Table 2) but we did not observe giant granules like those occasionally described [27]. The shape and morphology were normal but patients B3 and B4 exhibited occasional elongated  $\alpha$ -granules. The mean number of both types of specific granules per platelet was significantly increased in our patients but their number per unit of platelet area was normal, indicating that the increase was proportional to

the platelet size. Platelet ultra structure in MYH9-RD has not been studied quantitatively except in isolated reports. In one patient, where the intraplatelet structures were analyzed by stereological morphometry, the number of  $\alpha$ -granules was slightly increased, while that of dense bodies was normal [22].

The OCS is made by tortuous invaginations of the cell membrane and it increases the total platelet surface interacting with plasma both for endocytosis and for secretion. Also, it facilitates the interchange between the deepest cell areas with the extracellular space [26]. Due to the irregular shape of the OCS channel sections, we used the area instead of the diameter to measure their size (Table 2). The total area occupied by the OCS with respect to the platelet area was significantly expanded in our patients, as it has been previously described [19,22]. The size of the individual channels was significantly but moderately larger in patients' platelets and their shape sometimes suggested that they were the result of fusion. However, unlike other descriptions [19], the channels had no content.

The DTS is formed by residual endoplasmic reticulum and its channels are thinner than these of the OCS. The channels are filled with a relatively dense amorphous material and they are the calcium storage site in platelets. DTS has calcium pump activity which is essential for maintaining low calcium concentration in cytoplasm keeping the cell in resting discoid shape. Also, DTS contains prostaglandin endoperoxide synthetase which synthetize prostaglandins [26,28]. The small channels of DTS were not suitable to be evaluated by morphometry but their appearance and quantity appeared normal in the patients' platelets. Like in control platelets, we observed a few number of OCS and DTS clusters in patients' platelets and the morphometry confirmed this observation (Table 2).

It is known that mixed membrane complexes, formed by OCS and DTS, are present in small proportion in normal platelets and they are not exclusive of these cells [26,29]. We found a significant increase of membrane complexes in the platelets of our patients, in number per platelet and even in number per unit of platelet area (Table 2, Figure 2), indicating that their increase exceeded that which would correspond to the increase of platelet size. The striking development of the membrane complexes has been observed in most published cases as a characteristic ultra structural trait of the MYH9-RD platelets [10,20-22,24,25,27]. Epstein [19] described the membrane complexes as a tight maze of interconnecting vesicles or tubules in platelets as well in megakaryocytes and he deduced that they were the same structures that had described by Jordan as "small regions composed of intricately folded membranes" [17]. Membrane complexes are formed by a close apposition of OCS and DTS although there is no physical communication between both types of channels [10,26]. They represent regulatory elements for platelet contractility through the interchanges between SCO and DTS and with the usually nearby cytoskeleton. It has been suggested that the role of these structures could be the transfer of signals from the cell surface to the DTS such as occurred with transverse tubules and sarcotubules of muscle cells [28]. However, the precise function of membrane complexes is currently unknown [26]. In MYH9 disorders, the membrane complexes are also increased in megakaryocytes where their

large development disturbs the distribution of the demarcation membranes [19, 29].

Among unspecific structures, mitochondria were significantly larger and increased both per platelet and per unit of platelet area in patients' platelets (Table 2). In previous reports, mitochondria have been described as normal even when they were measured morphometrically [22]. Lipid droplets are known to be present in normal platelets in a small proportion [30]. They are cellular storage sites of lipids, mainly neutral fats, and, as corpuscular structures, they are suitable to be measured. The lipid droplets in our patients were normal in size and in number per unit of platelet area and they only show a proportional increase of its number per platelet (Table 2, Figure 2). Glycogen is a particulate substance regularly observed in platelets by ultra structure both as single particles and relatively large masses of irregular shape [26]. We measured the total area of the glycogen masses with respect to the platelet area and we found that they were significantly enlarged in our patients (Table 2, Figure 2). The MYH9-RD platelets that had been studied by stereological morphometry also showed a marked increase in glycogen masses [22]. We did not find any hypothesis that would explain why mitochondria and glycogen masses, both related to energy metabolism, were so developed in platelets of MYH9-RD patients.

Mutations of *MYH9* gene lead to abnormal NMMHC-IIA which is essential for platelet and megakaryocyte mechanical and contractile functions. Activated myosin assembles into contractile filaments through the myosin heavy chain and interacts mainly with central actin filaments playing a central role in the cytoskeletal function. Abnormal NMMHC-IIA leads to a modification in the composition and in the agonist-induced reorganization of the platelet cytoskeleton [3,4]. The most impaired functions derived from the mutated NMMHC-IIA in platelets are shape change, adhesion and outside-in signaling whereas aggregation and secretion seem to be less affected [3,4,15, 19,27]. In megakaryocytes, the anomaly disturbs the organization of the cytoplasm, the formation and stabilization of the demarcation membranes and the proplatelet formation [5-7]. As a consequence, MYH9-RD megakaryocytes generate a smaller number of platelets which are of larger in size

Platelet granules could also be influenced by the abnormal NMMHC-IIA, not only in the secretion process, in which the actomyosin cytoskeleton is implicated [26], but also in their biogenesis. Platelet granules are generated from multivesicular bodies and later they obtain their components by biosynthesis or by endocytosis [31]. Cell membrane remodeling is essential for this occurs and it requires the application of mechanical forces from the actomyosin cytoskeleton [32]. Despite this complex interactions between platelet granules and cytoskeleton, our ultra structural morphometric study only found a significant but moderate increase in the size of these structures.

The increase of mixed membrane complexes was clearly stated in the patients' platelets through morphometric measures. The striking presence of membrane complexes in MYH9-RD platelets has some theoretical consequences such as the increase of membrane surface interacting with the exterior, with the additional contribution of the expanded isolated channels of OCS, the increase of the DTS components and the increase of

the interactions between OCS and DTS. Further studies would be needed to investigate these functional aspects of the platelet membrane complexes and their potential clinical implications.

## CONCLUSION

Our morphometric study on platelet ultra structure in MYH9-RD confirmed several findings previously described such as the larger size and rounder shape of platelets and the prominent development of OCS and mixed membrane complexes. Moreover, we found that the size of  $\alpha$ -granules and dense bodies was enlarged, and the amounts of mitochondria and glycogen, both related to cell energy metabolism, were significantly increased. We discussed of all these findings in relation to platelet cytoskeleton defects due to the mutated NMMHCIIA.

## REFERENCES

1. Balduini CL, Pecci A, Savoia A. Recent advances in the understanding and management of MYH9-related inherited thrombocytopenias. *Br J Haematol.* 2011; 154: 161-174.
2. Savoia A, De Rocco D, Pecci A. MYH9 gene mutations associated with bleeding. *Platelets.* 2017; 28: 312-315.
3. Canobbio I, Noris P, Pecci A, Balduini A, Balduini CL, Torti M. Altered cytoskeleton organization in platelets from patients with MYH9-related disease. *J Thromb Haemost.* 2005; 3: 1026-1035.
4. Léon C, Eckly A, Hechler B, Aleil B, Freund M, Ravanat C, et al. Megakaryocyte-restricted MYH9 inactivation dramatically affects hemostasis while preserving platelet aggregation and secretion. *Blood.* 2007; 110: 3183-3191.
5. Eckly A, Strassel C, Freund M, Cazenave JP, Lanza F, Gachet C, et al. Abnormal megakaryocyte morphology and proplatelet formation in mice with megakaryocyte-restricted MYH9 inactivation. *Blood.* 2009; 113: 3182-3189.
6. Pecci A, Malara A, Badalucco S, Bozzi V, Torti M, Balduini CL, et al. Megakaryocytes of patients with MYH9-related thrombocytopenia present an altered proplatelet formation. *Thromb Haemost.* 2009; 102: 90-96.
7. Chen Y, Boukour S, Milloud R, Favier R, Saposnik B, Schlegel N, et al. The abnormal proplatelet formation in MYH9-related macrothrombocytopenia results from an increased actomyosin contractility and is rescued by myosin IIA inhibition. *J Thromb Haemost.* 2013; 11: 2163-2175.
8. Godwin HA, Ginsburg AD. May-Hegglin anomaly: a defect in megakaryocyte fragmentation? *Br J Haematol.* 1974; 26: 117-128.
9. Fabris F, Casonato A, Randi ML, Girolami A. Plasma and platelet beta-thromboglobulin levels in patients with May-Hegglin anomaly. *Haemostasis.* 1980; 9: 126-130.
10. White JG, Sauk JJ. The organization of microtubules and microtubule coils in giant platelet disorders. *Am J Pathol.* 1984; 116: 514-522.
11. Greinacher A, Mueller-Eckhardt C. Hereditary types of thrombocytopenia with giant platelets and inclusion bodies in the leukocytes. *Blut.* 1990; 60: 53-60.
12. Pujol-Moix N, Kelley MJ, Hernández A, Muñiz-Diaz E, Español I. Ultrastructural analysis of granulocyte inclusions in genetically confirmed MYH9-related disorders. *Haematologica.* 2004; 89: 330-337.
13. Pujol-Moix N, Hernández A, Escolar G, Español I, Martínez-Brotóns F, Mateo J. Platelet ultrastructural morphometry for diagnosis of partial delta-storage pool disease in patients with mild platelet dysfunction

- and/or thrombocytopenia of unknown origin. A study of 24 cases. *Haematologica*. 2000; 85: 619-626.
14. Dong F, Li S, Pujol-Moix N, Luban NL, Shin SW, Seo JH, et al. Genotype-phenotype correlation in MYH9-related thrombocytopenia. *Br J Haematol*. 2005; 130: 620-627.
  15. Noris P, Spedini P, Belletti S, Magrini U, Balduini CL. Thrombocytopenia, giant platelets, and leukocyte inclusion bodies (May-Hegglin anomaly): clinical and laboratory findings. *Am J Med*. 1998; 104: 355-360.
  16. Salvadó Piera J, Pujol-Moix N. "Coulter STKS" y macrotrombocitopenia. Descripción de un patrón característico muy útil para su detección. *Biol Clin Hematol*. 1995; 17: 140-144.
  17. Jordan SW, Larsen WE. Ultrastructural Studies of the May-Hegglin anomaly. *Blood*. 1965; 25: 921-932.
  18. Lusher JM, Schneider J, Mizukami I, Evans RK. The May-Hegglin anomaly: platelet function, ultrastructure and chromosome studies. *Blood*. 1968; 32: 950-961.
  19. Epstein CJ, Sahud MA, Piel CF, Goodman JR, Bernfield MR, Kushner JH, et al. Hereditary macrothrombocytopenia, nephritis and deafness. *Am J Med*. 1972; 52: 299-310.
  20. Hansen MS, Behnke O, Pedersen NT, Videbaek A. Megathrombocytopenia associated with glomerulonephritis, deafness and aortic cystic medianecrosis. *Scand J Haematol*. 1978; 21: 197-205.
  21. Peterson LC, Rao KV, Crosson JT, White JG. Fechtner syndrome - a variant of Alport's syndrome with leukocyte inclusions and macrothrombocytopenia. *Blood*. 1985; 65: 397-406.
  22. Heynen MJ, Blockmanns D, Verwilghen RL, Vermynen J. Congenital macrothrombocytopenia, leucocyte inclusions, deafness and proteinuria: functional and electron microscopic observations on platelets and megakaryocytes. *Br J Haematol*. 1988; 70: 441-448.
  23. Noris P, Klersy C, Gresele P, Giona F, Giordano P, Minuz P, et al. Platelet size for distinguishing between inherited thrombocytopenias and immune thrombocytopenia: a multicentric, real life study. *Br J Haematol*. 2013; 162: 112-119.
  24. Pujol-Moix N, Muñoz-Diaz E, Moreno-Torres ML, Hernandez A, Madoz P, Domingo A. Sebastian platelet syndrome. Two new cases in a Spanish family. *Ann Hematol*. 1991; 62: 235-237.
  25. Pujol-Moix N, Muñoz-Diaz E, Hernandez A, Romero MA, Puig J. Fechtner syndrome variant: a new family with mild Alport's manifestations. *Br J Haematol*. 1994; 86: 686-687.
  26. White JG. Platelet structure. In: Michelson AD. *Platelets* (Third Edition). Academic Press. Amsterdam, 2013. 117-144.
  27. Hamilton RW, Shaikh BS, Ottie JN, Storch AE, Saleem A, White JG. Platelet function, ultrastructure, and survival in the May-Hegglin anomaly. *Am J Clin Pathol*. 1980; 74: 663-668.
  28. White JG, Gerrard JM. Ultrastructural features of abnormal blood platelets. A review. *Am J Pathol*. 1976; 83: 589-632.
  29. Breton-Gorius J. Development of two distinct membrane systems associated in giant complexes in pathological megakaryocytes. *Ser Haematol*. 1975; 8: 49-67.
  30. Jean G, Racine L, Marx R, Gautier A. [On the presence of neutral fats in normal and pathological human thrombocytes]. *Thromb Diath Haemorrh*. 1963; 9: 1-11.
  31. Heijnen H, van der Sluijs P. Platelet secretory behaviour: as diverse as the granules ... or not? *J Thromb Haemost*. 2015; 13: 2141-2151.
  32. Milberg O, Shitara A, Ebrahim S, Masedunskas A, Tora M, Tran DT, et al. Concerted actions of distinct nonmuscle myosin II isoforms drive intracellular membrane remodeling in live animals. *J Cell Biol*. 2017; 216: 1925-1936.

#### Cite this article

Pujol-Moix N, Español I, Hernández A, Vázquez-Santiago M, Souto JC, et al. (2017) Platelet Ultrastructural Morphology and Morphometry in 10 Patients with MYH9-Related Disease. *J Hematol Transfus* 5(2): 1065.